ChemPubSoc Europe

DOI: 10.1002/cmdc.201500461

CHEMMEDCHEM Communications

SPECIAL ISSUE

# Structural Re-engineering of the α-Helix Mimetic JY-1-106 into Small Molecules: Disruption of the Mcl-1–Bak-BH3 Protein–Protein Interaction with 2,6-Di-Substituted Nicotinates

Brandon Drennen,[a] Jacob A. Scheenstra,[a] Jeremy L. Yap,[a] Lijia Chen,[a] Maryanna E. Lanning,[a] Braden M. Roth,[b] Paul T. Wilder,[b, c] and Steven Fletcher*[a, c]

The disruption of aberrant protein–protein interactions (PPIs) with synthetic agents remains a challenging goal in contemporary medicinal chemistry but some progress has been made. One such dysregulated PPI is that between the anti-apoptotic Bcl-2 proteins, including myeloid cell leukemia-1 (Mcl-1), and the α-helical Bcl-2 homology-3 (BH3) domains of its pro-apoptotic counterparts, such as Bak. Herein, we describe the discovery of small-molecule inhibitors of the Mcl-1 oncoprotein based on a novel chemotype. Particularly, re-engineering of our α-helix mimetic JY-1-106 into 2,6-di-substituted nicotinates afforded inhibitors of comparable potencies but with significantly decreased molecular weights. The most potent inhibitor 2-(benzyloxy)-6-(4-chloro-3,5-dimethylphenoxy)nicotinic acid (**1 r**: $K_i = 2.90$ μM) likely binds in the p2 pocket of Mcl-1 and engages R263 in a salt bridge through its carboxylic acid, as supported by 2D $^{1}H$–$^{15}N$ HSQC NMR data. Significantly, inhibitors were easily accessed in just four steps, which will facilitate future optimization efforts.

Apoptosis, or programmed cell death, ensures normal tissue homeostasis, and its dysregulation can lead to several human pathologies, including cancer.[1,2] Whilst the extrinsic apoptosis pathway is initiated through the activation of cell-surface receptors, the intrinsic apoptosis pathway occurs at the mitochondrial outer membrane and is governed by the binding interactions between pro- and anti-apoptotic Bcl-2 family proteins.[3] The anti-apoptotic proteins, which include Bcl-2, Bcl-$x_L$, Bcl-w, Bcl-A1 and Mcl-1, bind to the α-helical Bcl-2 homology-3 (BH3) domains of pro-apoptotic proteins, which include Bax, Bak and Bim, effectively neutralizing them and inhibiting apoptosis.[4,5] In many cancers, the anti-apoptotic Bcl-2 proteins are upregulated, and in this way the cancer cells can evade apoptosis.[2] Accordingly, synthetic small-molecule strategies to inhibit the Bcl-2 proteins have been adopted as a new avenue for cancer therapy.[6]

The *Mcl-1* gene is frequently overexpressed in human cancers,[7] including lung,[8] breast,[9] pancreatic,[10] cervical cancers,[11] as well as leukemia.[12] Importantly, genetic mouse models have shown that Mcl-1 is involved in tumor initiation and development.[13] Thus, for these reasons, Mcl-1 has emerged as an attractive target for anticancer therapy. Indeed, in the last few years, several groups, including ours, have developed inhibitors of Mcl-1,[14,15] which span a variety of scaffolds such as indoles,[16–18] 5-phenylsalicylates, 1-hydroxynaphthalenes,[19] 1-hydroxy-2-naphthoates[20] and tetrahydroquinolines,[21] all of which contain a carboxylic acid to bind R263. In addition, the neutral pyrogallol MIM1[22] and an 8-hydroxyquinoline derivative[23] have also been described as Mcl-1 inhibitors, and it is possible these neutral agents still engage R263 through hydrogen bond(s). However, no Mcl-1 inhibitor has advanced to the clinic. Finally, it is especially noteworthy that Leverson and colleagues recently reported that their highly potent and selective Mcl-1 inhibitor A-1210477 demonstrates on-target cellular effects, thus establishing for the first time that Mcl-1 is a viable cell target for the development of novel anticancer therapies.[24]

In addition to conventional small-molecule strategies, Mcl-1 inhibitors have been fashioned through the structural mimicry of BH3 α-helical domains.[25–31] However, such "α-helix mimetics" targeting Bcl-2 proteins have not advanced to the clinic,[32–34] and this may be due to their high molecular weights (MWs), which contravene Lipinski's rule as they are typically in excess of 500, and/or a lack of specificity. α-Helix mimetics typically reproduce functionality on only one face of the α-helix, specifically the *i*, *i*+3/4 and *i*+7 positions. These are often rather hydrophobic molecules, and their inhibitory activities might stem from nonspecific hydrophobic effects, at least in part. We believe that the recognition properties of an α-helix mimetic can be enhanced by mimicking additional faces of the α-helix.[28,31,35] On the other hand, a successful α-helix mimetic might be used as the inspiration from which

[a] *B. Drennen, J. A. Scheenstra, Dr. J. L. Yap, L. Chen, M. E. Lanning, Dr. S. Fletcher*
*Department of Pharmaceutical Sciences*
*University of Maryland School of Pharmacy*
*Baltimore, MD 21201 (USA)*
*E-mail: sfletcher@rx.umaryland.edu*

[b] *Dr. B. M. Roth, Dr. P. T. Wilder*
*Department of Biochemistry and Molecular Biology*
*Center for Biomolecular Therapeutics*
*University of Maryland School of Medicine*
*Baltimore, MD 21201 (USA)*

[c] *Dr. P. T. Wilder, Dr. S. Fletcher*
*University of Maryland Greenebaum Cancer Center*
*Baltimore, MD 21201 (USA)*

Supporting information for this article is available on the WWW under http://dx.doi.org/10.1002/cmdc.201500461.

SPECIAL ISSUE This article is part of a Special Issue on Protein–Protein Interactions. To view the complete issue, visit: http://onlinelibrary.wiley.com/doi/10.1002/cmdc.v11.8/issuetoc.


© 2016 Wiley-VCH Verlag GmbH & Co. KGaA, Weinheim

a more traditional small molecule could be realized. Along these lines, we herein describe the structural re-engineering of our α-helix mimetic JY-1-106[26,27] into a series of 2,6-di-substituted nicotinates that are equipotent at inhibiting Mcl-1 but bear significantly decreased MWs.

BH3 α-helices recognize Mcl-1 through binding four hydrophobic sub-pockets p1-p4 via conserved hydrophobic residues at the *i*, *i*+3/4 and *i*+7 and *i*+11 positions along one face of the α-helix. Additionally, a conserved aspartate on the opposing face of the α-helix binds R263. As an example, the co-crystal structure of Mcl-1–Bim-BH3 is given in Figure 1 A, and the key residues of the Bim-BH3 α-helix are shown more clearly in Figure 1 B. We recently reported the discovery of the BH3 α-helix mimetic JY-1-106 (Figure 1 C), which is a dual Bcl-$x_L$/Mcl-1 inhibitor (Bcl-$x_L$: $K_i = 179 \pm 24$ nM; Mcl-1: $K_i = 1.79 \pm 0.15$ μM).[26,27] The isopropyl groups of JY-1-106 were designed to target the p2, p3 and p4 pockets of Mcl-1, whilst the role of the carboxylic acid group was to enhance compound solubility rather than target any residue in particular.

We hypothesized that the central picolinamide subunit of JY-1-106 could serve as a scaffold to generate synthetically accessible, small-molecule inhibitors of Mcl-1. We postulated that retaining but modifying the substitution at both positions flanking the pyridine nitrogen of the picolinamide fragment might still permit binding to both the p2 and p3 pockets, whilst relocation of the carboxylic acid *meta* to the nitrogen atom might also allow the formation of a salt bridge with R263. One such simple molecule, **1 a**, is shown in Figure 2. Computational modeling of **1 a** with Mcl-1 (after ligand extraction, Mcl-1 coordinates from PDB ID: 4HW2[16]) was conducted with GOLD (version 5.2.2), and a low-energy docked solution is given in Figure 3. The small molecule–Mcl-1 crystal structure 4HW2 was selected for docking studies because our synthetic ligand is now more akin to a traditional small molecule rather than an α-helix or a conventional α-helix mimetic.[32] According to the modeling results, the phenyl ring snuggly fits into the p2 pocket (partially obscured) and the isobutyl group is pointed towards the p3 pocket, docking nicely into a new pocket bounded by A227 and M231 not found in crystal structures of Mcl-1 with BH3 ligands.[16] Furthermore, a weak salt bridge (3.9 Å) is detected between the carboxylic acid and R263, although given the plasticity[16] of the hydrophobic groove of Mcl-1, as revealed by multiple crystal structures (e.g. PDB ID: 4HW2,[16] 4HW3,[16] 4HW4,[16] 3WIX[36]), we envisage stronger interactions between the acid and R263 may be possible. With this modeling data in hand, we then prepared a library of analogues of compound **1 a** in which we modified the alkoxy ($R^1O$) and aryloxy ($R^2O$) groups.

Accordingly, 2,6-dichloronicotinic acid (**2**) was regioselectively alkoxylated *ortho* to the acid with various $R^1OH$ alcohols to afford **3** using chemistry recently developed in our laboratory.[37] Incidentally, the ability to selectively control the displacement of the two chlorines in 2,6-dichloronicotinic acid directly facilitated the development of a new α-helix mimetic.[38] Subsequent esterification of **3** was accomplished with thionyl chloride and methanol to yield methyl esters **4**. A second $S_NAr$ reaction was effected with phenols $R^2OH$ to deliver compounds **5**, or thiophenols $R^2SH$ to yield compounds **6**, which were finally saponified to furnish target molecules **1 a**–**1 r** and **7 a**–**7 d**, respectively, in just four steps (Scheme 1).

In order to quantify the abilities of compounds to inhibit Mcl-1, a fluorescence polarization competition (FPC) assay was

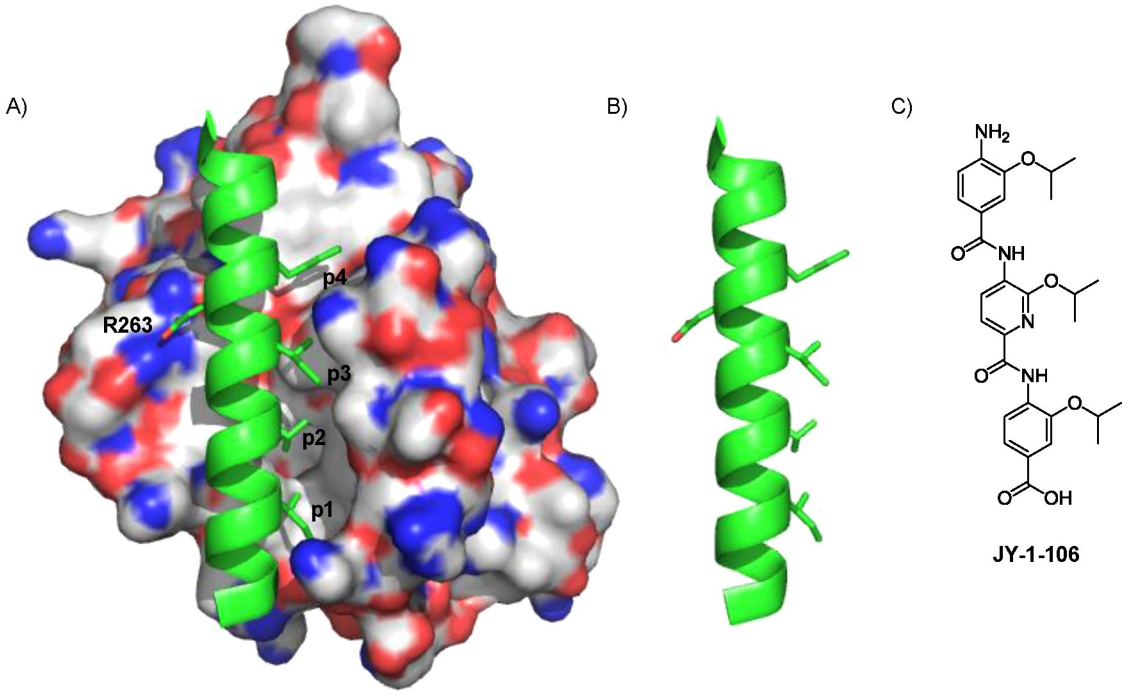


**Figure 1.** A) Structure of Mcl-1–Bim–BH3 (PDB ID: 4HW4[16]). Mcl-1 colored by atom type: carbon = grey; blue = nitrogen; red = oxygen; yellow = sulfur. Bim–BH3 α-helix colored in green. Key residues and binding pockets on Mcl-1 are shown in black. B) Key residues of the Bim–BH3 α-helix. C) The α-helix mimetic JY-1-106.


© 2016 Wiley-VCH Verlag GmbH & Co. KGaA, Weinheim

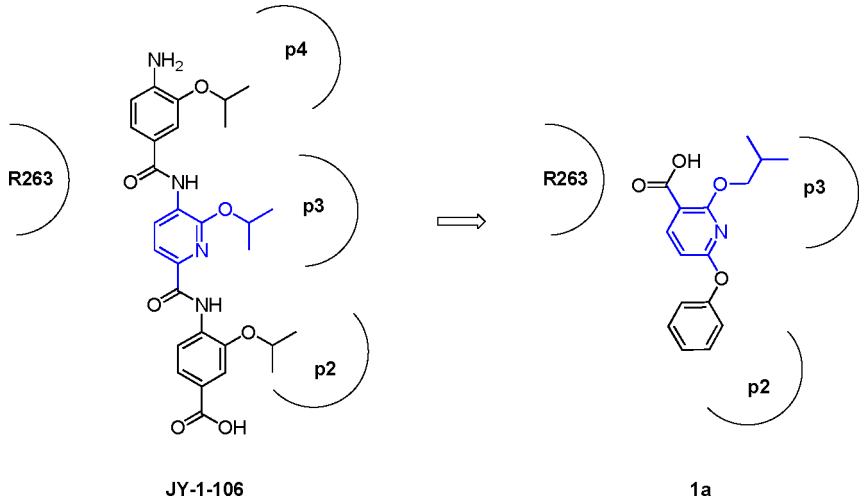


**Figure 2.** Reduction of the α-helix mimetic JY-1-106 into small molecule **1 a**. Labels in half-bubbles refer to Mcl-1 residues and subpockets.

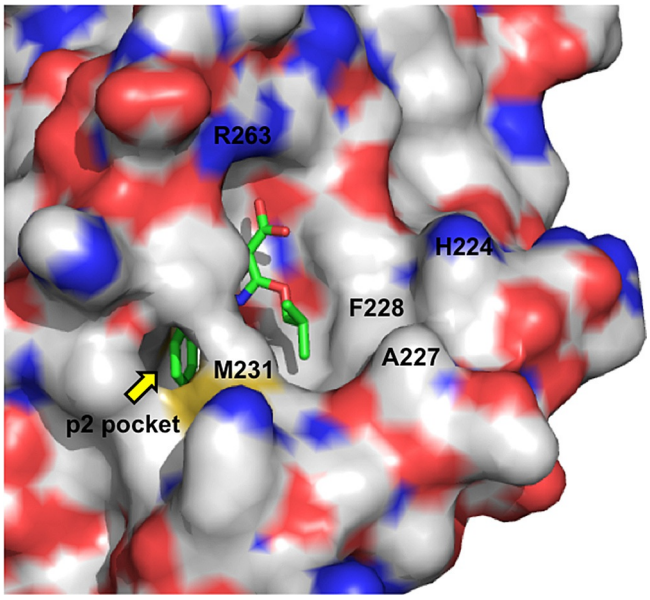


**Figure 3.** Low-energy GOLD docking solution of **1 a** (green carbon atoms; heteroatoms colored by atom type) bound to Mcl-1 (coordinates from PDB ID: 4HW2[16]). Mcl-1 (surface representation) is colored by atom type: carbon = grey; blue = nitrogen; red = oxygen; yellow = sulfur.

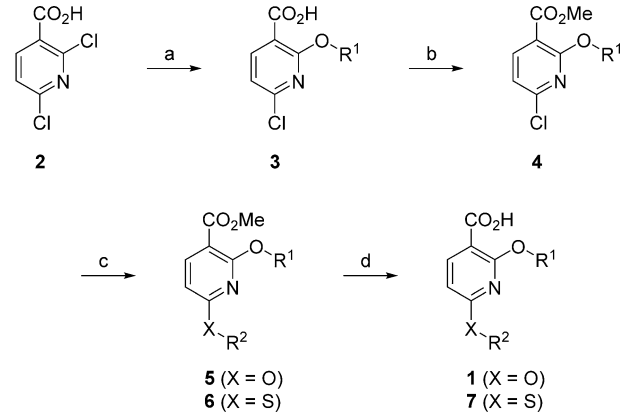


**Scheme 1.** *Reagents and conditions*: a) $R^1OH$, NaH, THF, 60 °C, 16 h; b) $SOCl_2$, MeOH, 60 °C, 3 h; c) $R^2OH$ or $R^2SH$, $K_2CO_3$, DMF, 100 °C, 72 h; d) $LiOH{\cdot}H_2O$, THF/MeOH/$H_2O$ (3:1:1), RT, 3 h.

employed in which the compounds competed with a fluorescein isothiocyanate (FITC)-labeled Bak-BH3 peptide for binding to Mcl-1$^{172-327}$. $IC_{50}$ data resulting from the analysis were converted to $K_i$ values using the Nikolovska–Coleska equation[39] and are given in Table 1. For further details, see the Experimental Section. The simplest compound (**1 a**) exhibited the weakest binding to Mcl-1 with a $K_i$ value of 261 μM. However, the introduction of halogens into the phenyl $R^2$ group resulted in improved inhibition, and the effect was cumulative, which can be seen by comparing the data for **1 c** and **1 e** with that for **1 f**. Indeed, **1 f** ($K_i$ = 6.69 μM) was almost 40-fold more potent than parent compound **1 a**. Naphthyl $R^2$ derivatives also proved better inhibitors of Mcl-1 over **1 a** with the 1-naphthyl derivative (**1 b**) superior to its regioisomer (**1 g**). Whilst substitution of the phenyl $R^2$ moiety with hydrophobic groups always enhanced the inhibitory activity over parent compound **1 a**, *para*-substitution led to the greatest increases in inhibition. For example, compare the data for 2-chlorophenyl (**1 c**) with 4-chlorophenyl (**1 e**) derivatives, and 3,5-dimethylphenyl (**1 k**) with 4-methylphenyl (**1 h**) derivatives. In every case, replacement of the $R^2$ ether oxygen (X group) with a sulfur atom (**7 a**–**7 d**) resulted in an improvement in inhibitory activity of between 2.5-fold and 12-fold. Compound **7 c** was the most potent of the thioether series with a $K_i$ value of 3.69 μM. Finally, we examined the effect of varying the $R^1$ group. As the size of the hydrophobic $R^1$ group was increased, the resulting inhibitor generally became more potent. In fact, **1 r** was the most potent compound of the entire series ($K_i$ = 2.90 μM).

Evidence for the direct binding of **1 r** to Mcl-1 was provided by heteronuclear NMR studies. 2D $^1H$–$^{15}N$ heteronuclear single quantum coherence (HSQC) spectra of [$^{15}N$]-labelled Mcl-1 were collected in the absence and presence of **1 r**. An overlay of the two spectra (Figure 4) revealed significant chemical shift changes, particularly for R263 and those residues located around the p2 pocket; those changes ≥0.3 ppm have been


© 2016 Wiley-VCH Verlag GmbH & Co. KGaA, Weinheim

**Table 1.** Mcl-1 structure–activity relationships of 2,6-di-substituted nicotinates. $IC_{50}$ data[a] from a fluorescence polarization competition assay with Mcl-1$^{172-371}$ and fluorescein isothiocyanate (FITC)-labeled Bak were converted to $K_i$ values using the Nikolovska–Coleska equation.[39]

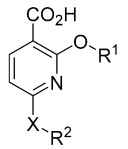


| Compd | $R^1$ | $R^2$ | X | $K_i$ [μM] | Compd | $R^1$ | $R^2$ | X | $K_i$ [μM] |
|---|---|---|---|---|---|---|---|---|---|
| **1a** |  | 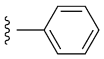 | O | 261 ± 33 | **1l** |  | 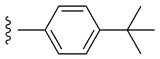 | O | 11.1 ± 2.3 |
| **1b** |  | 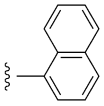 | O | 40.0 ± 4.2 | **7a** |  | 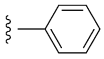 | S | 48.1 ± 7.1 |
| **1c** |  | 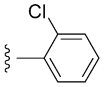 | O | 72.8 ± 4.6 | **7b** |  | 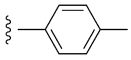 | S | 7.11 ± 0.78 |
| **1d** |  | 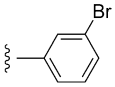 | O | 55.6 ± 4.9 | **7c** |  | 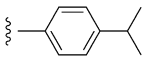 | S | 3.69 ± 0.17 |
| **1e** |  | 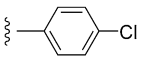 | O | 39.8 ± 2.1 | **7d** |  | 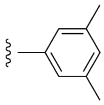 | S | 50.3 ± 3.7 |
| **1f** |  | 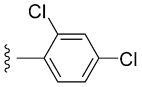 | O | 6.69 ± 0.71 | **1m** |  | 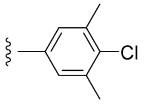 | O | 25.4 ± 1.4 |
| **1g** |  | 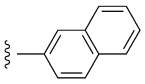 | O | 59.6 ± 3.4 | **1n** |  | 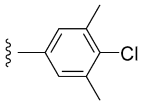 | O | 26.9 ± 8.6 |
| **1h** |  | 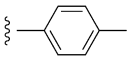 | O | 87.8 ± 18.4 | **1o** |  | 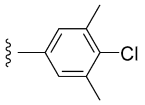 | O | 20.0 ± 1.1 |
| **1i** |  | 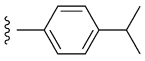 | O | 47.0 ± 10.6 | **1p** |  | 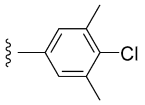 | O | 4.58 ± 1.20 |
| **1j** |  | 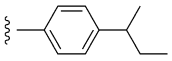 | O | 12.7 ± 1.3 | **1q** | 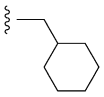 |  | O | 4.62 ± 0.77 |
| **1k** |  |  | O | 123 ± 16 | **1r** |  |  | O | 2.90 ± 1.24 |

[a] Data represent the mean ± SD of three biological replicates, each performed in triplicate.

mapped onto the Mcl-1 crystal structure PDB ID: 4HW2[16] and are shown in red in Figure 5.

Overall, larger and more hydrophobic $R^1$ and $R^2$ groups afforded greater inhibition of Mcl-1. This finding may be due to more efficient interactions with the hydrophobic p2 pocket, which is supported by the HSQC NMR data. The inhibitory activity was enhanced further still by replacing the $R^2$ phenyl ether oxygen with a sulfur atom, which can be rationalized by the greater hydrophobicity of sulfur over oxygen coupled with the idea that the $R^2$ group is directed into the hydrophobic p2 pocket. In addition, the carboxylic acid of the inhibitors was critical to activity since the methyl ester derivative of **1r** exhib-


© 2016 Wiley-VCH Verlag GmbH & Co. KGaA, Weinheim

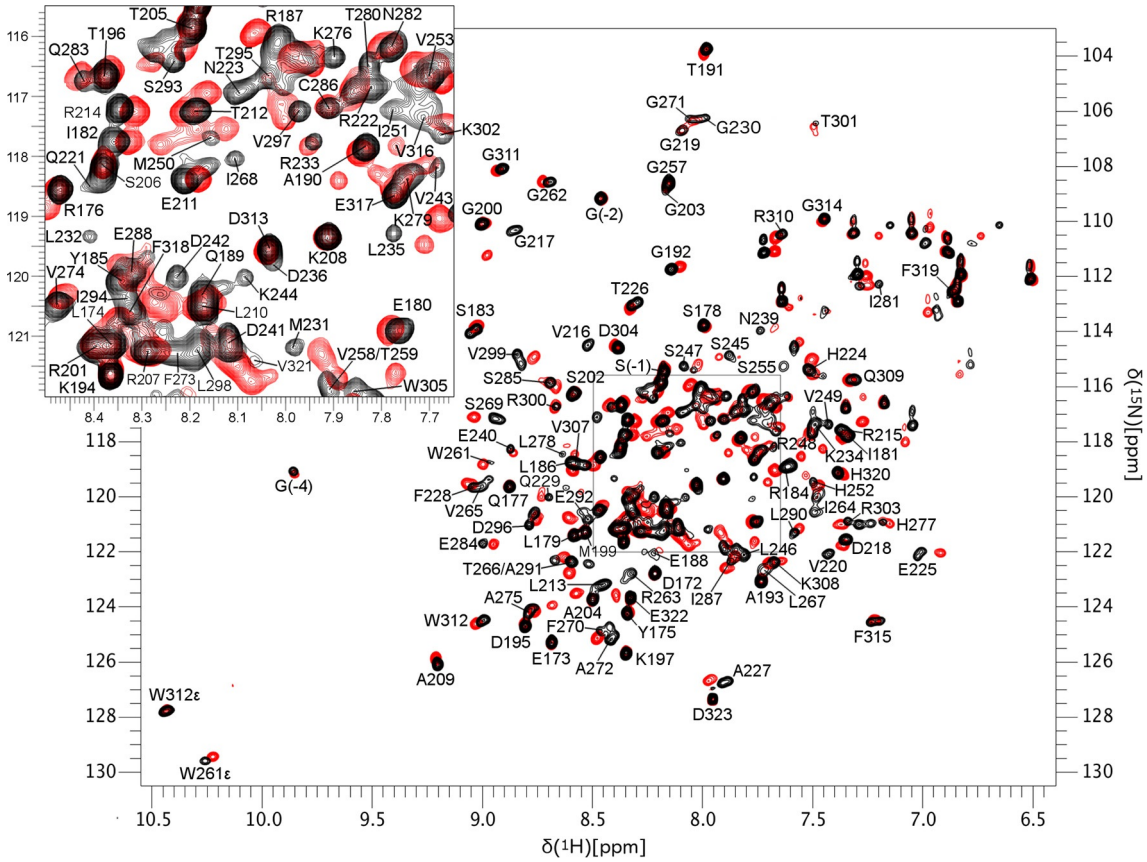


**Figure 4.** $^{1}H$–$^{15}N$ heteronuclear single-quantum correlation (HSQC) spectra overlay of apo-Mcl-1 (black) and **1 r**-bound Mcl-1 (red).

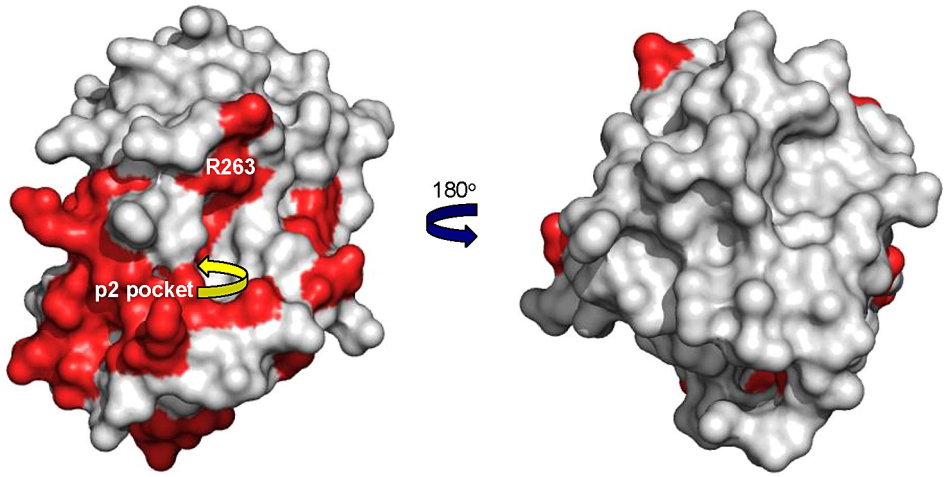


**Figure 5.** $^{1}H$–$^{15}N$ chemical shift perturbations $\geq$0.3 ppm of Mcl-1 in the presence of **1 r** (red) mapped onto the Mcl-1 crystal structure (PDB ID: 4HW2[16]).

ited no effect on the Mcl-1–Bak-BH3 PPI (data not shown), which is consistent with the design rationale wherein the carboxylic acid was proposed to form a salt bridge with R263.

Many of the inhibitors described in the present work exhibited similar $K_i$ values to the α-helix mimetic JY-1-106 ($K_i$ = 1.79 μM), yet they have much lower MWs. Indeed, the two most potent compounds (**7 c** and **1 r**) are about two-thirds the mass of JY-1-106, bringing their MWs within the threshold proposed by Lipinski (MW < 500). Furthermore, their lipophilicities are also significantly decreased. For example, the cLog*P* and cLog*D* values (pH 7.4) for JY-1-106 are 7.37 and 4.32, respectively, whilst the corresponding values for **1 r** are 6.11 and 2.98, respectively. Finally, we evaluated the selectivity profile of **1 r** for Bcl-2 family members. As shown in Figure 6, the $IC_{50}$ values for **1 r** against Mcl-1 and Bcl-$x_L$ were 11.35 ± 4.85 μM and 31.53 ± 6.19 μM, respectively, which correspond to $K_i$ values of 2.90 ± 1.24 μM and 2.04 ± 0.40 μM, respectively. It is noteworthy that the 10-fold Bcl-$x_L$-selectivity of JY-1-106 has been almost completely eroded upon its transformation into small-molecule nicotinates; future work will focus on the acquisition


© 2016 Wiley-VCH Verlag GmbH & Co. KGaA, Weinheim

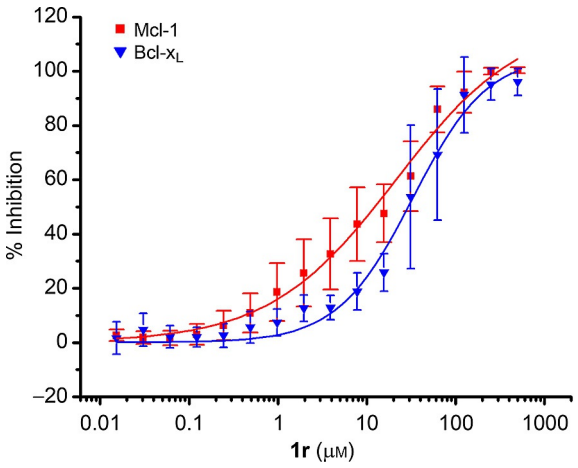


**Figure 6.** Inhibition of Mcl-1 (■) and Bcl-$x_L$ (▼) by compound **1r**, as determined by a fluorescent polarization competition (FPC) assay with fluorescein isothiocyanate (FITC)-labeled Bak. Data points are the mean and error bars the standard deviation of three biological replicates performed in triplicate.

of crystal structures of **1r** with Mcl-1 and Bcl-$x_L$ to assist in further enhancement in affinity and selectivity for Mcl-1.

In summary, using our previously reported α-helix mimetic JY-1-106 as a starting point, we have developed a new family of readily accessible Mcl-1 inhibitors based on a 2,6-di-substituted nicotinic acid core. HSQC NMR data supported the hypothesis that the $R^1$ group and/or the $R^2$ group probe(s) into the p2 pocket, whilst the carboxylic acid likely engages R263 through a salt bridge, although the exact binding mode remains unknown at this time. It is noteworthy that our most potent compounds are about as potent as the α-helix mimetic JY-1-106 yet exhibit significantly decreased MW and cLog*D* values. Additional structure–activity studies are currently underway, which, as well as enhancing compound affinity, aim to gain a better understanding of the specific binding mode and how this can be exploited towards achieving selectivity for specific Bcl-2 family members of anti-apoptotic proteins.

## Experimental Section

**Supporting Information**: Complete protocols for both chemical syntheses and biological methods together with characterization data are presented in the Supporting Information available via Wiley Online Library.

**Molecular docking**: Compound **1a** was first MM2 energy minimized in ChemBio3D Ultra 14.0. The 4HW2[16] PDB file was uploaded into GOLD (version 5.2.2), all the appropriate hydrogen atoms were added, water molecules were removed, and then the ligand was extracted. The binding site was defined as 10 Å about the side chain sulfur of Met231; no further constraints were used.

**First $S_NAr$ Reaction (general procedure A)**: Alcohol $R^1OH$ (5 equiv) was dissolved in anhydrous THF (0.10 M), and the solution was cooled to 0 °C then NaH (5 equiv; 60% dispersion in mineral oil) was slowly added. The reaction mixture was stirred for 30 min at 0 °C before 2,6-dichloronicotinic acid (1 equiv) was added portionwise, and then the mixture was heated overnight at 60 °C in an oil bath. The next day, the reaction was cooled to 0 °C, quenched with brine (1 mL), then concentrated to approximately 10 mL. The reaction mixture was partitioned between $CH_2Cl_2$ and 1 M aq HCl (the aqueous layer was pH ~ 2). The organic layer was collected, and the aqueous layer was extracted with $CH_2Cl_2$ twice further. The organic layers were combined, dried with $Na_2SO_4$, filtered and concentrated to yield the crude *ortho*-substituted nicotinic acid, which was used without further purification.

**Esterification (general procedure B)**: The *ortho*-substituted nicotinic acid (1 equiv) was dissolved in MeOH (0.10 M), and the solution was cooled to 0 °C. Thionyl chloride (3 equiv) was slowly added, and then the mixture was refluxed for 3 h. The reaction mixture was concentrated to dryness. The crude ester was adsorbed onto silica gel, then purified by flash column chromatography (eluent: hexane/EtOAc, 4:1).

**Second $S_NAr$ Reaction (general procedure C)**: The methyl ester (1 equiv) was dissolved in DMF (0.10 M). The appropriate phenol ($R^2OH$) or thiophenol ($R^2SH$) (4 equiv) was added to the solution followed by $K_2CO_3$ (3 equiv). The reaction was heated at 100 °C for 72 h. The reaction was partitioned between EtOAc and $H_2O$. The organic layer was isolated and washed repeatedly (5×) with $H_2O$. The organic layer was then collected, dried with $Na_2SO_4$, filtered and concentrated under vacuum. The crude material was adsorbed onto silica gel, then purified by flash column chromatography (eluent: hexane/EtOAc, 4:1).

**Saponification (general procedure D)**: The *o,p*-di-substituted nicotinate (1 equiv) was dissolved in a 3:1:1 solution of THF/MeOH/$H_2O$ (0.10 M). LiOH·$H_2O$ (4 equiv) was added, and the reaction mixture was stirred at RT for 3 h. If necessary, the reaction volume was decreased to approximately 10 mL, then partitioned between $Et_2O$ and $H_2O$. The ethereal layer was discarded, and then the aqueous layer was acidified to pH 2 with 0.1 M HCl, then extracted twice with $CH_2Cl_2$. The organic layer was collected, the aqueous layer was extracted once more with $CH_2Cl_2$, then the organic extractions were combined, dried with $Na_2SO_4$, filtered and concentrated to produce the *o,p*-di-substituted nicotinic acid. All final molecules were deemed to exhibit > 95% purities by HPLC and were not purified further.

**Fluorescence polarization experiments**: Fluorescence polarization experiments were conducted using a PHERAstar FS multimode microplate reader (BMG LabTech) equipped with two photomultiplier tubes (PMTs) for simultaneous measurements of the perpendicular and parallel fluorescence emission. For the competition assay, inhibitors were titrated into a solution of Mcl-$1^{172–327}$ (or Bcl-$x_L^{2–212}$), and the fluorescently labeled Bak-BH3 peptide FITC-Ahx-GQVGRQLAIIGDDINR-$CONH_2$ (hereafter "FITC-Bak"), where FITC is fluorescein isocyanate and Ahx is 6-aminohexanoyl linker. Regression analysis was carried out using Origin (OriginLab, Northampton, USA) to fit the data to the Hill equation to determine the initial binding affinity ($K_d$) and the $IC_{50}$ in the FPC assay. $K_d$ values for the FITC–Bak peptide to Mcl-1 and Bcl-$x_L$ were 33.8 ± 0.50 nM and 6.67 ± 0.05 nM, respectively. For the fluorescence polarization competition titrations, an equation derived by Nikolovska–Coleska et al. was used to calculate the $K_i$ values from the $IC_{50}$ data.[39] All experiments were run in three biological replicates, each performed in triplicate.

**NMR Spectroscopy**: 2D $^1H$–$^{15}N$ HSQC spectra were collected with 200 indirect points and 32 scans at 25 °C with a Bruker AVANCE 800 MHz NMR spectrometer (800.27 MHz for protons) equipped with pulsed-field gradients, four frequency channels, and triple resonance, *z*-axis gradient cryogenic probes. A one-second relaxation delay was used, and quadrature detection in the indirect dimensions was obtained with states–time proportional phase incremen-


© 2016 Wiley-VCH Verlag GmbH & Co. KGaA, Weinheim

tation (TPPI) phase cycling; initial delays in the indirect dimensions were set to give zero- and first-order phase corrections of 90° and −180°, respectively.[40,41] Data were processed using the processing program nmrPipe on Linux workstations.[42] All proton chemical shifts are reported with respect to the residue $H_2O$ or HDO signal, taken to be 4.658 ppm relative to external trimethylsilyl propanoic acid (TSP) (0.0 ppm) at 37 °C. The $^{15}N$ chemical shifts were indirectly referenced using the zero-point frequency ratio of 0.10132905 for $^{1}H$–$^{15}N$ at 37 °C, as previously described.[43,44] Uniformly $^{15}N$-labeled Mcl-1 was used to collect 2D $^{1}H$–$^{15}N$-fast HSQC spectra of Mcl-1 with and without compound to detect changes in the backbone $^{15}N$ and $^{1}H$ resonances of Mcl-1 due to the direct interaction with compound **1r**, which itself was initially dissolved in 100% [$D_6$]DMSO.[45] The NMR samples contained 61.9 μM $^{15}N$-labeled Mcl-1, 20 mM 4-(2-hydroxyethyl)-1-piperazineethanesulfonic acid (HEPES), pH 6.8, 36.4 mM NaCl, 0.20 mM $NaN_3$, 2.2 mM dithiothreitol (DTT), 4.2% DMSO, 20% $D_2O$. A concentrated solution of **1r** was added in excess to a final protein:ligand ratio of 1:2 (i.e., 123.8 μM).

## Acknowledgements

*The authors thank the University of Maryland School of Pharmacy (Baltimore, USA) and the Center for Biomolecular Therapeutics (Baltimore, USA) for financially supporting this research, and acknowledge receipt of a US National Institutes of Health Training Grant at the Chemical-Biology Interface (T32GM066706).*

**Keywords:** cancer · JY-1-106 · Mcl-1 · nicotinic acid · protein–protein interactions

[1] D. Hanahan, R. A. Weinberg, *Cell* **2000**, *100*, 57–70.
[2] J. M. Adams, S. Cory, *Oncogene* **2007**, *26*, 1324–1337.
[3] G. Kroemer, L. Galluzzi, C. Brenner, *Physiol. Rev.* **2007**, *87*, 99–163.
[4] S. Cory, J. M. Adams, *Nat. Rev. Cancer* **2002**, *2*, 647–656.
[5] R. J. Youle, A. Strasser, *Nat. Rev. Mol. Cell Biol.* **2008**, *9*, 47–59.
[6] J. T. Opfermann, *FEBS J.* **2016**, DOI: 10.1111/febs.13472.
[7] R. Beroukhim, C. H. Mermel, D. Porter, G. Wei, S. Raychaudhuri, J. Donovan, J. Barretina, J. S. Boehm, J. Dobson, M. Urashima, K. T. Mc Henry, R. M. Pinchback, A. H. Ligon, Y.-J. Cho, L. Haery, H. Greulich, M. Reich, W. Winckler, M. S. Lawrence, B. A. Weir et al., *Nature* **2010**, *463*, 899–905.
[8] L. Song, D. Coppola, S. Livingston, W. D. Cress, E. B. Haura, *Cancer Biol. Ther.* **2005**, *4*, 267–276.
[9] Q. Ding, X. He, W. Xia, J.-M. Hsu, C.-T. Chen, L.-Y. Li, D.-F. Lee, J.-Y. Yang, X. Xie, J.-C. Liu, M.-C. Hung, *Cancer Res.* **2007**, *67*, 4564–4571.
[10] Y. Miyamoto, R. Hosotani, M. Wada, J. U. Lee, T. Koshiba, K. Fujimoto, S. Tsuji, S. Nakajima, R. Doi, M. Kato, Y. Shimada, M. Imamura, *Oncology* **1999**, *56*, 73–82.
[11] T. Zhang, C. Zhao, L. Luo, H. Zhao, J. Cheng, F. Xu, *Med. Oncol.* **2012**, *29*, 1985–1991.
[12] M. H. Andersen, J. C. Becker, P. Thor Straten, *Leukemia* **2005**, *19*, 484–485.
[13] S. P. Glaser, E. F. Lee, E. Trounson, P. Bouillet, A. Wei, W. D. Fairlie, D. J. Izon, J. Zuber, A. R. Rappaport, M. J. Herold, W. S. Alexander, S. W. Lowe, L. Robb, A. Strasser, *Genes Dev.* **2012**, *26*, 120–125.
[14] J. Belmar, S. W. Fesik, *Pharmacol. Ther.* **2015**, *145*, 76–84.
[15] L. Chen, M. E. Lanning, S. Fletcher, *Austin J. Anal. Pharm. Chem.* **2015**, *1*, 1015.
[16] A. Friberg, D. Vigil, B. Zhao, R. N. Daniels, J. P. Burke, P. M. Garcia-Barrantes, D. Camper, B. A. Chauder, T. Lee, E. T. Olejniczak, S. W. Fesik, *J. Med. Chem.* **2013**, *56*, 15–30.
[17] J. P. Burke, Z. Bian, S. Shaw, B. Zhao, C. M. Goodwin, J. Belmar, C. F. Browning, D. Vigil, A. Friberg, D. V. Camper, O. W. Rossanese, T. Lee, E. T. Olejniczak, S. W. Fesik, *J. Med. Chem.* **2015**, *58*, 3794–3805.
[18] M. Bruncko, L. Wang, G. S. Sheppard, D. C. Phillips, S. K. Tahir, J. Xue, S. Erickson, S. Fidanze, E. Fry, L. Hasvold, G. J. Jenkins, S. Jin, R. A. Judge, P. J. Kovar, D. Madar, P. Nimmer, C. Park, A. M. Petros, S. H. Rosenberg, M. L. Smith et al., *J. Med. Chem.* **2015**, *58*, 2180–2194.
[19] F. A. Abulwerdi, C. Liao, A. S. Mady, J. Gavin, C. Shen, T. Cierpicki, J. A. Stuckey, H. D. H. Showalter, Z. Nikolovska-Coleska, *J. Med. Chem.* **2014**, *57*, 4111–4133.
[20] M. E. Lanning, W. Yu, J. L. Yap, J. Chauhan, L. Chen, E. Whiting, L. S. Pidugu, T. Atkinson, H. Bailey, W. Li, B. M. Roth, L. Hynicka, K. Chesko, E. A. Toth, P. Shapiro, A. D. MacKerell, Jr., P. T. Wilder, S. Fletcher, *Eur. J. Med. Chem.* **2016**, DOI: 10.1016/j.ejmech.2016.02.006.
[21] L. Chen, P. T. Wilder, B. Drennen, J. Tran, B. M. Roth, K. Chesko, P. Shapiro, S. Fletcher, *Org. Biomol. Chem.* **2016**, DOI: 10.1039/C5OB02063H.
[22] N. A. Cohen, M. L. Stewart, E. Gavathiotis, J. L. Tepper, S. R. Bruekner, B. Koss, J. T. Opferman, L. D. Walensky, *Chem. Biol.* **2012**, *19*, 1175–1186.
[23] D. J. Richard, R. Lena, T. Bannister, N. Blake, W. E. Pierceall, N. E. Carlson, C. E. Keller, M. Koenig, Y. He, D. Minond, J. Mishra, M. Cameron, T. Spicer, P. Hodder, M. H. Cardone, *Bioorg. Med. Chem.* **2013**, *21*, 6642–6649.
[24] J. D. Leverson, H. Zhang, J. Chen, S. K. Tahir, D. C. Phillips, J. Xue, P. Nimmer, S. Jin, M. Smith, Y. Xiao, P. Kovar, A. Tanaka, M. Bruncko, G. S. Sheppard, L. Wang, S. Gierke, L. Kategaya, D. J. Anderson, C. Wong, J. Eastham-Anderson et al., *Cell Death Dis* **2015**, *6*, e1590.
[25] A. Kazi, J. Sun, K. Doi, S.-S. Sung, Y. Takahashi, H. Yin, J. M. Rodriguez, J. Becerril, N. Berndt, A. D. Hamilton, H.-G. Wang, S. M. Sebti, *J. Biol. Chem.* **2011**, *286*, 9382–9392.
[26] J. L. Yap, X. Cao, K. Vanommeslaeghe, K.-Y. Jung, C. Peddaboina, P. T. Wilder, A. Nan, A. D. MacKerell, W. R. Smythe, S. Fletcher, *Org. Biomol. Chem.* **2012**, *10*, 2928–2933.
[27] X. Cao, J. L. Yap, M. K. Newell-Rogers, C. Peddaboina, W. Jiang, H. T. Papaconstantinou, D. Jupitor, A. Rai, K.-Y. Jung, R. P. Tubin, W. Yu, K. Vanommeslaeghe, P. T. Wilder, A. D. MacKerell, Jr., S. Fletcher, R. W. Smythe, *Mol. Cancer* **2013**, *12*, 42.
[28] K.-Y. Jung, K. Vanommeslaeghe, M. E. Lanning, J. L. Yap, C. Gordon, P. T. Wilder, A. D. MacKerell, S. Fletcher, *Org. Lett.* **2013**, *15*, 3234–3237.
[29] H. Moon, W. S. Lee, M. Oh, H. Lee, J. H. Lee, W. Im, H.-S. Lim, *ACS Comb. Sci.* **2014**, *16*, 695–701.
[30] A. Barnard, K. Long, H. L. Martin, J. A. Miles, T. A. Edwards, D. C. Tomlinson, A. Macdonald, A. J. Wilson, *Angew. Chem. Int. Ed.* **2015**, *54*, 2960–2965.
[31] M. E. Lanning, P. T. Wilder, H. Bailey, B. Drennen, M. Cavalier, L. Chen, J. L. Yap, M. Raje, S. Fletcher, *Org. Biomol. Chem.* **2015**, *13*, 8642–8646.
[32] V. Azzarito, K. Long, N. S. Murphy, A. J. Wilson, *Nat. Chem.* **2013**, *5*, 161–173.
[33] M. Lanning, S. Fletcher, *Future Med. Chem.* **2013**, *5*, 2157–2174.
[34] H. Moon, H.-S. Lim, *Curr. Opin. Chem. Biol.* **2015**, *24*, 38–47.
[35] M. E. Lanning, S. Fletcher, *Biology* **2015**, *4*, 540–555.
[36] Y. Tanaka, K. Aikawa, G. Nishida, M. Homma, S. Sogabe, S. Igaki, Y. Hayano, T. Sameshima, I. Miyahisa, T. Kawamoto, M. Tawada, Y. Imai, M. Inazuka, N. Cho, Y. Imaeda, T. Ishikawa, *J. Med. Chem.* **2013**, *56*, 9635–9645.
[37] J. L. Yap, K. Hom, S. Fletcher, *Tetrahedron Lett.* **2011**, *52*, 4172–4176.
[38] B. Drennen, A. D. MacKerell, Jr., S. Fletcher, *Tetrahedron Lett.* **2015**, *56*, 6819–6822..
[39] Z. Nikolovska-Coleska, R. Wang, X. Fang, H. Pan, Y. Tomita, P. Li, P. P. Roller, K. Krajewski, N. G. Saito, J. A. Stuckey, S. Wang, *Anal. Biochem.* **2004**, *332*, 261–273.
[40] D. Marion, P. C. Driscoll, L. E. Kay, P. T. Wingfield, A. Bax, A. M. Gronenborn, G. M. Clore, *Biochemistry* **1989**, *28*, 6150–6156.
[41] A. Bax, M. Ikura, *J. Biomol. NMR* **1991**, *1*, 99–104.
[42] F. Delaglio, S. Grzesiek, G. W. Vuister, G. Zhu, J. Pfeifer, A. Bax, *J. Biomol. NMR* **1995**, *6*, 277–293.
[43] A. S. Edison, F. Abildgaard, W. M. Westler, E. S. Mooberry, J. L. Markley, *Meth. Enzymol.* **1994**, *239*, 3–79.
[44] S. Spera, M. Ikura, A. Bax, *J. Biomol. NMR* **1991**, *1*, 155–165.
[45] S. Mori, C. Abeygunawardana, M. O. Johnson, P. C. van Zijl, *J. Magn. Reson. B* **1995**, *108*, 94–98.

Received: October 8, 2015
Revised: November 23, 2015
Published online on February 4, 2016


© 2016 Wiley-VCH Verlag GmbH & Co. KGaA, Weinheim